Remote Sensing of Environment 208 (2018) 1–14

Contents lists available at ScienceDirect

Remote Sensing of Environment

journal homepage: www.elsevier.com/locate/rse

Comparison of airborne laser scanning and digital stereo imagery for characterizing forest canopy gaps in coastal temperate rainforests

Joanne C. White[a,*], Piotr Tompalski[b], Nicholas C. Coops[b], Michael A. Wulder[a]

[a] Canadian Forest Service, Pacific Forestry Center, Natural Resources Canada, 506 West Burnside Road, Victoria, BC V8Z 1M5, Canada
[b] Faculty of Forestry, University of British Columbia, 2424 Main Mall, Vancouver, BC V6T 1Z4, Canada

A R T I C L E I N F O

Keywords:
Forest structure
Seral stage
Habitat
Gap surveys
ALS
DAP
Canopy gaps
Gap size frequency distribution

A B S T R A C T

Forest canopy gaps play an important role in forest dynamics. Airborne laser scanning (ALS) data provide demonstrated capacity to systematically and accurately detect and map canopy gaps over large forest areas. Digital aerial photogrammetry (DAP) is emerging as an alternative, lower-cost source of three-dimensional information for characterizing forest structure and modelling forest inventory attributes. In this study we compared the relative capacities of ALS and DAP data to map canopy gaps in a complex coastal temperate rainforest on Vancouver Island, British Columbia, Canada. We applied fixed- and variable-height threshold approaches for gap detection using both ALS and DAP data, and validated outcomes using independent data derived via visual image interpretation. Overall accuracies for ALS-derived gaps were 96.50% and 89.50% for the fixed- and variable-height threshold approaches respectively, compared to 59.50% and 50.00% for the DAP-derived gaps, with DAP data having large errors of omission (> 88%). We found that 70% of ALS-derived gaps were identified in old seral stage stands (age > 250 years), while 65% of DAP-derived gaps were located in early seral stage stands (age < 40 years). For the DAP data, gap detection accuracy was 80% in early seral stands, compared to 50% in old seral stands. In contrast, ALS detection accuracy varied by only ~6% between early and old seral stages. We compared detected gaps using a variety of metrics and found significant differences in the number and average size of gaps detected using ALS and DAP data. Using the fixed-height threshold, the ALS data identified 16 times more gaps and 6.5 times more gap area than the DAP data, with a mean ALS-derived gap size that was half that of the DAP data. The average amount of overlap between ALS- and DAP-detected gaps was 13.26% and 42.90% for the variable and fixed thresholds, respectively. We attribute these differences in gap detection to the nature of the DAP data itself, which characterizes primarily the outer canopy envelope, as well as to the confounding effects of canopy complexity and related occlusions and shadows on image matching algorithms. We conclude that DAP data do not provide analogous results to ALS data for canopy gap detection and mapping in coastal temperate rainforests, and that ALS data enable markedly superior accuracy and detailed gap characterizations.

1. Introduction

Natural disturbances play an important role in forest ecosystems. Some disturbances, such as wildfire (e.g. Burton et al., 2008) or insects (e.g. Safranyik et al., 2010), can impact large areas over relatively short time frames. In contrast, the mortality of single trees or small groups of trees create openings or gaps within the continuous forest canopy that are either devoid of trees or contain trees that are markedly smaller than their immediate neighbours (Runkle, 1982). Canopy gaps play an important role in the ecological processes in natural forests and influence forest structure, particularly in mature and old stands (Spies et al., 1988). Gaps influence tree recruitment and regeneration success (Gray and Spies, 1996; Yamamoto, 2000; Muscolo et al., 2014), play a role in the maintenance of biodiversity (Gray et al., 2012), and can provide a matrix of preferred forage species for ungulates (Harestad, 1985; Massé and Côté, 2012; Tahtinen et al., 2014). In unmanaged coastal temperate forests of British Columbia, Canada, canopy gaps are the primary agent influencing forest composition and structure (Lertzman et al., 1996; Daniels and Gray, 2006). In this environment, gaps result in enhanced growth responses (Stan and Daniels, 2010, 2014). Lertzman et al. (1996) distinguished between ephemeral developmental gaps caused by tree mortality and branch fall, and more persistent gaps, which result from edaphic or topographic conditions, such as streams or rock outcroppings. By definition, canopy gaps are considered localized and discrete, and are not part of an "open-ended" system such as a wetland or a large burned area. While edaphic gaps contribute to openness of

* Corresponding author.
E-mail address: joanne.white@canada.ca (J.C. White).

https://doi.org/10.1016/j.rse.2018.02.002
Received 17 May 2017; Received in revised form 24 January 2018; Accepted 7 February 2018

the forest canopy and to landscape forest structure, they are not considered significant contributors to forest dynamics (Lertzman et al., 1996).

In the study of canopy gaps, both the spatial and temporal variation in the formation of canopy gaps is of interest (Lertzman et al., 1996). However, landscape-level spatial assessments of canopy gaps are often constrained by gap detection and mapping methods, which have primarily been ground-based measurements at sample locations (Schliemann and Bockheim, 2011). Given the level of effort and expense required to obtain ground-based measurements, the areas covered by these surveys are often small and not spatially contiguous. An improved understanding of the temporal variation in gap formation processes has also been limited by the lack of time series data to enable such investigations (Lertzman et al., 1996), and by the difficulties associated with repeat measurements. Conventional gap surveys often involve some form of transect sampling, as the accurate delineation of gap perimeters (determined by vertically projecting the outline of peripheral trees) is challenging (St-Onge et al., 2014), and research has demonstrated significant differences in gap size estimates using different field-based measurement methods (de Lima, 2005). Runkle (1992) identified the potential of aerial photography for mapping canopy gaps, and subsequent work by Fox et al. (2000) compared the accuracy of canopy gap maps generated from ground surveys to those generated from manual interpretation of high resolution (1:15,000) air photos. The authors found that maps generated from air photo interpretation were more accurate, with the latter having an omission rate of only 4.7% compared to 25.6% for the ground survey; however, although the air photos enabled a more synoptic detection and mapping of canopy gaps, they could not provide the same detailed information on the characteristics of the vegetation within the gaps, as would be provided by a ground survey (Fox et al., 2000).

In a review of contemporary literature for actual and potential methods for detecting canopy gaps, Runkle (1992) was prescient in identifying the capacity of future technologies (Runkle, 1992, p. 5):

> "Measurement of actual canopy heights on a regular grid system throughout a stand is another technique for gap surveys. Such a mapped grid provides a more accurate view of variation in canopy structure than a simple gap–non-gap dichotomy. It also clearly locates large gaps and gives a reasonable estimate of the fraction of land area in gaps as the proportion of grid points in gaps."

The capability to which Runkle (1992) was referring is now afforded by airborne laser scanning data (ALS; also referred to as airborne LiDAR), an active remote sensing technology that measures the 3-dimensional distribution of vegetation within forest canopies (Lefsky et al., 1999). ALS data also enable the detailed characterization of terrain under forest canopy with sub-metre accuracy (Reutebuch et al., 2003; Næsset, 2015) and likewise the accurate estimation of plot and stand canopy heights over large areas (Andersen et al., 2006). Indeed, ALS measures of canopy height are becoming the benchmark against which other measures are evaluated (White et al., 2016).

More recently, the capacity to derive detailed canopy surface characterization through an image matching photogrammetric workflow has emerged as a less costly alternative to ALS data (Baltsavias, 1999; Leberl et al., 2010). Commonly referred to as digital aerial photogrammetry or DAP, image-based point clouds are generated using image-matching algorithms that operate in stereo or multi-image matching modes, depending on the image acquisition parameters and degree of image overlap. The emergence of image-based point clouds have been enabled by advances in digital camera systems (increased overlap and improved radiometry) and computational power (Leberl et al., 2010) and numerous image matching approaches and algorithms have been developed (Gruen, 2012, Remondino et al., 2014). However, to date there has been limited benchmarking of acquisition parameters (Bohlin et al., 2012; Nurminen et al., 2013; Puliti et al., 2016) and image matching algorithms (Kukkonen et al., 2017; Granholm et al., 2017; Ullah et al., 2017) in forest environments. Moreover, very few image matching algorithms are designed specifically to operate on forest canopies (Baltsavias et al., 2008), which are particularly challenging targets for image matching algorithms because of shadows (Baltsavias, 1999), which increase with decreasing solar elevations (Honkavaara et al., 2012).

An accurate canopy height model (CHM) can be generated from an image-based point cloud when used in concert with a detailed ALS-derived digital terrain model (DTM) (St-Onge et al., 2008; Bohlin et al., 2012). In a review of the utility of image-based point clouds for forest inventory applications in 2013, White et al. (2013) noted that at the time of their review, there were very few studies that compared the performance of DAP and ALS data (i.e. Bohlin et al., 2012; Järnstedt et al., 2012). Subsequently, several studies have been published that have directly compared the performance of ALS and DAP for the estimation of a basic suite of forest inventory attributes such as height, basal area, and volume across a range of forest environments (e.g. Vastaranta et al., 2013; Pitt et al., 2014; Gobakken et al., 2014; White et al., 2015; Puliti et al., 2016; Bohlin et al., 2017; Rahlf et al., 2017; Hawryło et al., 2017). Using an area-based approach (Næsset, 2002), these studies have demonstrated that ALS and DAP provide comparable outcomes for inventory attributes across a range of forest environments—primarily because both technologies are capable of accurately characterizing canopy heights, which strongly influence the subsequent estimation of attributes such as volume (St-Onge et al., 2008).

The potential utility of airborne laser scanning data for detecting canopy gaps was first identified using airborne laser profiling systems in the mid-1980s (Nelson et al., 1984; Aldred and Bonner, 1985). Since that time, research across a range of boreal, temperate, and tropical forest environments has demonstrated the capabilities of ALS data for detecting and mapping canopy gaps (Table 1). These studies have used ALS data to characterize canopy gaps over very large areas (> 100,000 ha), enabling insights into landscape-level variations in gap size and frequency (Asner et al., 2013), a key information need identified in the ecological literature (e.g., Lertzman et al., 1996). Moreover, time series of ALS data have been used to quantify changes in the size and shape of canopy gaps over time (Vepakomma et al., 2008, 2011, 2012). The majority of studies have used the ALS-derived canopy height model (CHM) with a fixed-height threshold for gap detection. Most studies have not reported gap detection accuracy (Table 1); however, those that have evaluated the accuracy of gap detection report overall accuracies ranging from 82% to 97%. Gaulton and Malthus (2010) compared the use of a relative height threshold on both an ALS-derived CHM and point cloud, finding that gap detection using the point cloud directly provided a slight increase in gap detection accuracy of 3.7%; however, the authors also identified that the use of the point cloud was "considerably more computationally demanding" and given the relatively modest gain in detection accuracy, may not be justified over large areas. We are aware of only one study that has examined the use of DAP data for mapping canopy gaps (Zielewska-Büettner et al., 2016, 2017). In this study, the authors used stereoscopic aerial imagery from 2009 and 2012, and evaluated gap detection results using independent, visual interpretation of the imagery; however, the authors did not directly compare the gaps detected with the DAP data to those detected with the ALS data.

Recent research in less complex forest environments has indicated that DAP may be less effective than ALS data for mapping small canopy openings (Vastaranta et al., 2013); however, the capacity of DAP for this purpose has yet to be fully studied and quantified, and a detailed comparison of the gaps generated from ALS and DAP has yet to be undertaken. There are fundamental differences in the way these two data sources characterize the canopy, with ALS pulses penetrating small openings in the canopy, and thereby capturing the vertical distribution of vegetation, whereas DAP data primarily characterizes only the outer canopy envelope, with image matching algorithms interpolating across

Table 1
Summary of studies that have used ALS data to map canopy gaps across a range of forest types (adapted from St-Onge et al., 2014).

Study	ALS data	Field data	Forest type	Location	CHM or point cloud	Approach	Results
Vepakomma et al. (2008)	Two ALS datasets (both leaf on): 1998 (0.03 pulses/m^2) and 2003 (0.19 pulses/m^2)	Ground sampling of 4 line transects.	Dominated by balsam fir with white spruce, black spruce, white birch, and trembling aspen.	Quebec, Canada (600 ha)	CHM (0.25 m resolution)	Fixed height threshold = 5 m; minimum gap size = 5 m^2	Overall accuracy of gap detection (2003 only) = 96.5%.
Zhang (2008)	ALS pulse density not reported; point spacing was 0.6 m cross-track and an average of 1 m along-track	Nine field sites were monitored to characterize gap changes from 1999 to 2004.	Mangrove forests	Everglades NP, Florida, USA (130 ha)	CHM (1 m resolution)	Fixed height threshold = 11 m; relative height threshold (35–40%); minimum gap size = 10 m^2	Accuracy of gap detection was assessed qualitatively (i.e. visually).
Gaulton and Malthus (2010)	Two ALS datasets: high density = 11.4 pulses/m^2 and low density = 1.2 pulses/m^2	All gap boundaries within each plot were surveyed using a Total Station.	Sitka spruce plantations	Three 1-ha plots (1 in Scotland; 2 in Wales) UK (3 ha)	CHM and point cloud. Results of using both were compared. Resolution of CHM was 0.5–1 m (varied by site)	Relative height threshold (66% of maximum canopy height), gaps detected on CHM and directly from the point cloud. Minimum gap size = 5 m^2	Overall accuracy of gap detection: from point cloud = 78.2%; from CHM = 74.5%
Vehmas et al. (2011)	ALS: 3.9 pulses/m^2	Field data used to validate gap class only.	Mature spruce forest	Koli National Park in eastern Finland (1000 ha)	CHM (0.5 m resolution)	Fixed height threshold = 5 m, minimum gap size 5 m^2 (following Vepakomma et al., 2008)	Gaps classified into 5 classes. Various gap characteristics calculated. Gap detection accuracy not reported.
Kane et al. (2011)	ALS: 1 pulse/m^2	48 study sites representing different stand structure classes	Douglas fir, western hemlock, western red cedar.	Cascade Range in Washington State, USA (11,200 ha)	CHM (1.5 m resolution)	Fixed height threshold = 3 m, minimum gap size = 9 m^2	Gap dynamics and various gap structure properties assessed. Gap detection accuracy not reported.
Vepakomma et al. (2012)	Multitemporal ALS data: 1998 = 0.3 pulses/m^2, 2003 = 3 pulses/m^2, 2007 = 7 pulses/m^2		Dominated by balsam fir with white spruce, black spruce, white birch, and trembling aspen.	Lake Duparquet, north-western Quebec, Canada (26 ha)	CHM (0.25 m)	Fixed height threshold = 5 m, minimum gap size of 5 m^2 (following Vepakomma et al., 2008)	Gap detection accuracy not reported. Gap dynamics analyzed with a focus on changes in gap shape and size over 9 year period.
Asner et al. (2013)	ALS: 2 pulses/m^2		Tropical rainforests	South-Peruvian Amazon (125,581 ha)	CHM (resolution not reported)	Two fixed height thresholds applied: 1 m and 20 m	Gaps size frequency analyzed for different land cover classes. Gap detection accuracy not reported.
Boyd et al. (2013)	ALS: 2.1 pulses/m^2		Tropical rainforests	South-Peruvian Amazon (142,500 ha)	CHM (1–2 m resolution)	Fixed height threshold = 2 m with a minimum area of 2 m^2	Canopy gaps size frequency distribution characterized with power law. Gap detection accuracy not reported.
Bonnet et al. (2015)	Two ALS datasets: leaf on and leaf off (both 21 pulses/m^2)	4 study sites, 50 × 50 m sample grid; 1140 points visited interpreted as "gap" or "not gap", field checked; 39 gaps mapped with dGPS	Uneven-aged broadleaved stands (oak, European beech, and birch).	Belgium, Europe (18,000 ha)	CHM (0.5 m resolution)	3 methods: thresholding (3 m) per-pixel supervised classification, per-object supervised classification. Minimum gap size = 50 m^2; classification done with Random Forest.	Gap detection accuracy = 82%; gap geometric accuracy analyzed with the gap area, main orientation, shape complexity index

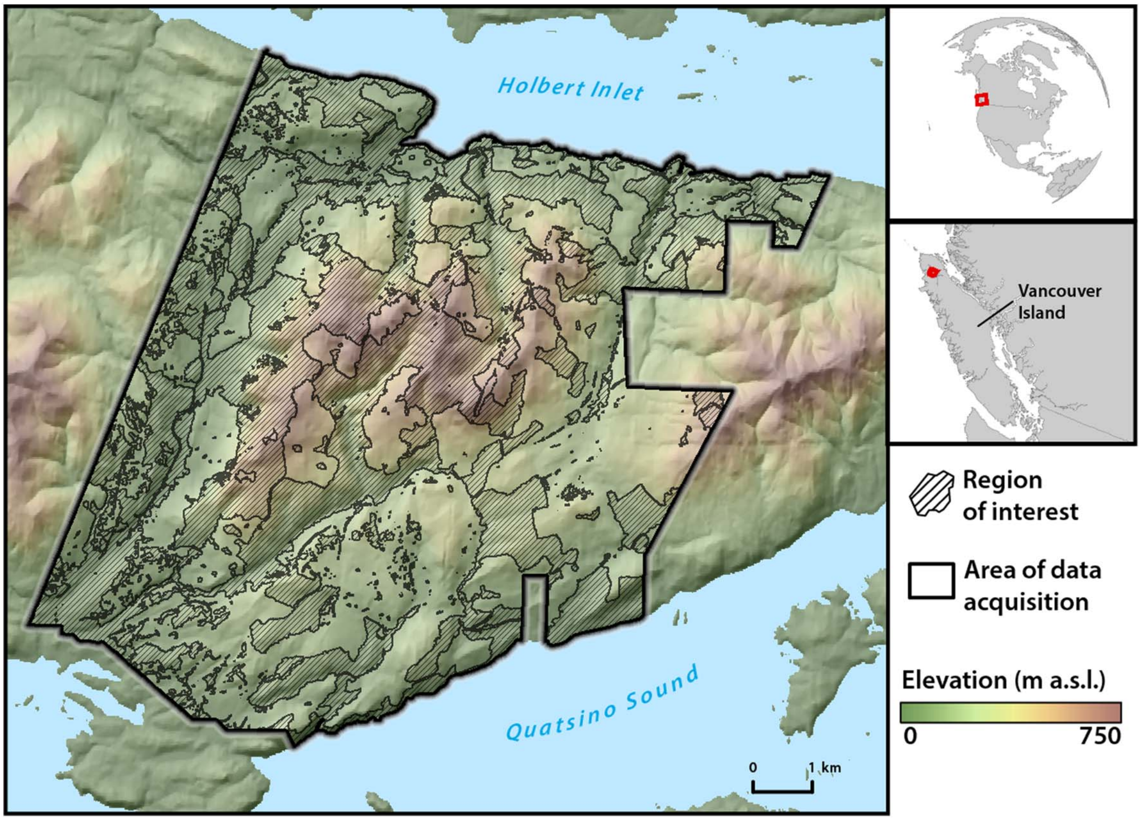

Fig. 1. Location of study area and region of interest (ROI) on Vancouver Island, British Columbia, Canada.

small gaps that are either occluded by other trees or in shadow (Baltsavias et al., 2008; St-Onge et al., 2014). In the stereo-matching scenario of the DAP data used in this study, a gap has only two opportunities to be "viewed" (and thereby matched). If one of the views of the gap is obstructed or in shadow, then the gap will not be captured in the image point cloud. Hirschmugl et al. (2007) demonstrate that a multi-image matching scenario (enabled by a 90% along-track image overlap) can significantly improve the detection of small canopy gaps and forest edges; however, the majority of imagery used for generating image-based point clouds in a forestry context (and reported in the published literature) are acquired with only a 60% along-track image overlap (White et al., 2015) and do not enable this multi-image matching scenario. As ALS data do not have the aforementioned limitations associated with DAP, we expected the ALS data to provide a more accurate characterization of canopy gaps in our coastal temperate rainforest study area. Differences in gap detection capacity between ALS and DAP can have implications for studies of gap dynamics that seek to monitor changes in gaps over time, wherein ALS data may be used to characterize gaps initially, with subsequent gap detection and mapping done at future points in time using DAP data. Thus, the degree to which these data sources convey similar information regarding the location and size of gaps must be understood. The objective of this study was therefore to quantify the differences in gap detection between ALS and DAP derived canopy gaps for a complex, coastal temperate rainforest on Vancouver Island, British Columbia to gain some insights on the relative capacity of DAP data for this application.

2. Methods

2.1. Study area

The study area is situated on the Pacific Northwest coast of North America on northern Vancouver Island, British Columbia, Canada, and covers approximately 8500 ha (Fig. 1). Located within the Coastal Western Hemlock submontane very wet maritime subzone (CWHvm1), the study area is characterized by high annual precipitation (2228 mm), mild winters, and cool summers (Meidinger and Pojar, 1991). The area receives little snow and has a long growing season. Elevation within the study area ranges from sea level to 662 m.

Vegetation in the study area is characterized as a highly productive temperate rainforest dominated by western hemlock (*Tsuga heterophylla*) and amabalis fir (*Abies amabilis*), with lesser amounts of western red cedar (*Thuja plicata*). A range of seral stages are found within the study area, with the old seral stage (> 250 years) representing the majority of the area (Table 2; B.C. Ministry of Forests and B.C. Ministry of Environment, Lands, and Parks). Large, natural, stand-initiating events are rare in these forests, resulting in an older, uneven-age forest with complex within-stand structure (Lertzman et al., 1997). Canopy

Table 2
Distribution of seral stages within the study area.

Seral stage	Age (years)	Proportion of study area (%)	Mean height (ALS)	Std deviation (ALS)	Mean height (DAP)	Std deviation (DAP)
Early	< 40	23.01	15.80	6.72	14.21	5.83
Mid	40≥ and < 80	5.93	26.93	9.83	25.85	8.92
Mature	≥80 and < 250	12.21	33.17	11.15	33.25	7.35
Old	≥250	58.86	27.58	12.87	29.39	8.50

Table 3
ALS acquisition parameters.

Parameter	Description
Sensor	ALTM3100EA
Aircraft speed	240 km/h
Data acquisition height	700 m a.g.l.
Swath width	323 m
Max scan angle	± 12.5°
Beam divergence	0.3 mrad
Wavelength	1064 nm
Overlap	75%
Pulse repetition rate	70 kHz
Scan frequency	65 Hz
Number of returns per pulse	4
Pulse density	11.6 pulses/m^2 [a] (SD = 4.3 pulses/m^2)

[a] Pulse density was calculated for 25 m × 25 m grid cells and averaged.

gaps play an important role in influencing forest structure and composition in these forests (Lertzman et al., 1996; Daniels and Gray, 2006).

The analysis area (hereafter referred to as the region of interest or ROI) was defined by excluding areas without high vegetation, including areas recently harvested. Those areas were defined based on their size (> 2 ha) *and* low canopy heights (< 10 m). Areas identified as "no data" in either the ALS or the DAP were also excluded. The final ROI was 4350 ha (Fig. 1).

2.2. Data

2.2.1. ALS data

ALS data were acquired in August and September of 2012 using an Optech ALTM3100EA scanning system from an altitude of approximately 700 m above ground level (Table 3). The average point density was 11.6 points/m^2. A Digital Terrain Model (DTM_{ALS}) with a spatial resolution of 1 m was created using ground returns and standard preprocessing routines following the methods of Axelsson (2000). Using first returns, a Digital Surface Model (DSM_{ALS}) was generated with a 1 m spatial resolution. The DSM_{ALS} and DTM_{ALS} were used to generate a 1 m canopy height model (CHM_{ALS}) representing normalized heights above ground. ALS processing was performed using LAStools software (version 161114).

2.2.2. DAP data

Digital imagery was acquired for the study area using a Vexcel UltraCamX camera in September 2012 (Table 4). The imagery was 4-band (RGB and NIR) with a 0.30 m ground sampling distance (GSD) and was acquired along 6 flight lines, with a minimum 60% along-track and 20% across-track overlap. We used the semi-global matching (SGM) algorithm (Hirschmüller, 2008), as implemented in the Remote Sensing Software Package Graz (RSG version 7.46.11) to generate dense image point clouds. As per Stepper et al. (2014), only along-track stereo pairs were used for image matching. In total there were 49 stereo pairs.

Table 4
DAP acquisition parameters.

Parameter	Description
Sensor	Vexcel UltraCamX
Data acquisition height	4228 m a.g.l.
Across-track overlap	20%
Along-track overlap	60% minimum
GSD	0.30 m
Cross-track field of view	55°
Along-track field of view	37°
Pixel size	7.2 µm
Point density	12.27 pts/m^2

Absolute orientation of the images was achieved during acquisition using onboard GPS and IMU data. The resulting point density of the image-based point cloud was 12.27 points/m^2. The output of the processing was a digital surface model (DSM_{DAP}) and canopy height model (CHM_{DAP}) both with a spatial resolution of 1 m.

2.3. Co-registration of the ALS and DAP data

An initial comparison of CHM_{ALS} and CHM_{DAP} revealed that there was a misalignment of the two datasets that could potentially influence gap detection results. The shift was not constant for the whole study area, but was consistent within each flight line of the aerial photo acquisition. Thus, co-registration of the ALS and DAP data was undertaken for each of the DAP flight lines using the following procedure. First, a 1-m resolution DSM was generated for each flight line independently using the DAP point clouds for that flight line. Second, each of the DSM_{DAP} layers was adjusted to align with the DSM_{ALS} using at least six ground control points (GCPs) distributed evenly across each DSM_{DAP}. Characteristic terrain features (e.g. road crossings), and distinctive tree crowns were used as GCPs. Special attention was given to areas of across-track image overlap, where transformation points were selected on overlapping DSM_{DAP} layers and the DSM_{ALS}. Finally, the adjusted individual DSM_{DAP} layers were then mosaicked and normalized to heights above ground using DTM_{ALS}. A revised canopy height model (CHM_{DAP}) was then generated from the DSM_{DAP} using the DTM_{ALS}. CHM_{DAP} and CHM_{ALS} were then differenced and compared, with summary measures (e.g. Pearson's R, RMSE) generated for the entire analysis area, and by seral stage.

2.4. Gap detection

The two most common methods for gap detection reported in the scientific literature are fixed and variable height thresholds (Table 1). We applied both of these approaches to CHM_{ALS} and CHM_{DAP} to compare outcomes between the two data sources and approaches. Fixed height thresholds are determined by the user who typically considers the ecological conditions relevant to the forest ecosystem in question, whereas variable height thresholds are determined relative to the height of the canopy surrounding a gap. For the fixed-height threshold approach, we defined a CHM pixel as a gap if it had a height < 3 m. The 3 m height threshold was adapted after Kane et al. (2011) who used this value in a similar environment of topographically variable, structurally diverse coastal temperate forests. We removed gaps that were < 5 m^2 and > 2 ha in size from further analysis.

For the variable-height threshold approach, gaps are detected using a variable height threshold that is determined by the relative height of the canopy drip line. The canopy drip line typically represents the maximum extent of the tree crown in coniferous forests (Gaulton and Malthus, 2010). Based on the method presented by Gaulton and Malthus (2010), we determined the relative height of the canopy drip line by manually measuring 50 randomly located trees in the ALS point clouds. The measurements included tree height and height to canopy drip line. The mean value of the proportion of the canopy drip line height to tree height was 0.64, and this value, which was similar to the 0.66 value used by Gaulton and Malthus (2010), was used in our analysis (Fig. 2). To determine the relative height threshold for each CHM pixel, we first generated a surface representing the maximum height of the canopy (top of canopy), by applying a moving maximum filter in a 11 × 11 pixel window. The filter size is a trade-off between preventing the top of canopy from falling within small gaps between trees, and maintaining the height variation in the stands. Each pixel in the CHM was then classified as a gap if its canopy height value was < 64% of the corresponding maximum height. As per the fixed-height threshold approach, gaps that were < 5 m^2 and > 2 ha were removed from further analysis.

We evaluated the degree of overlap between the DAP- and ALS-

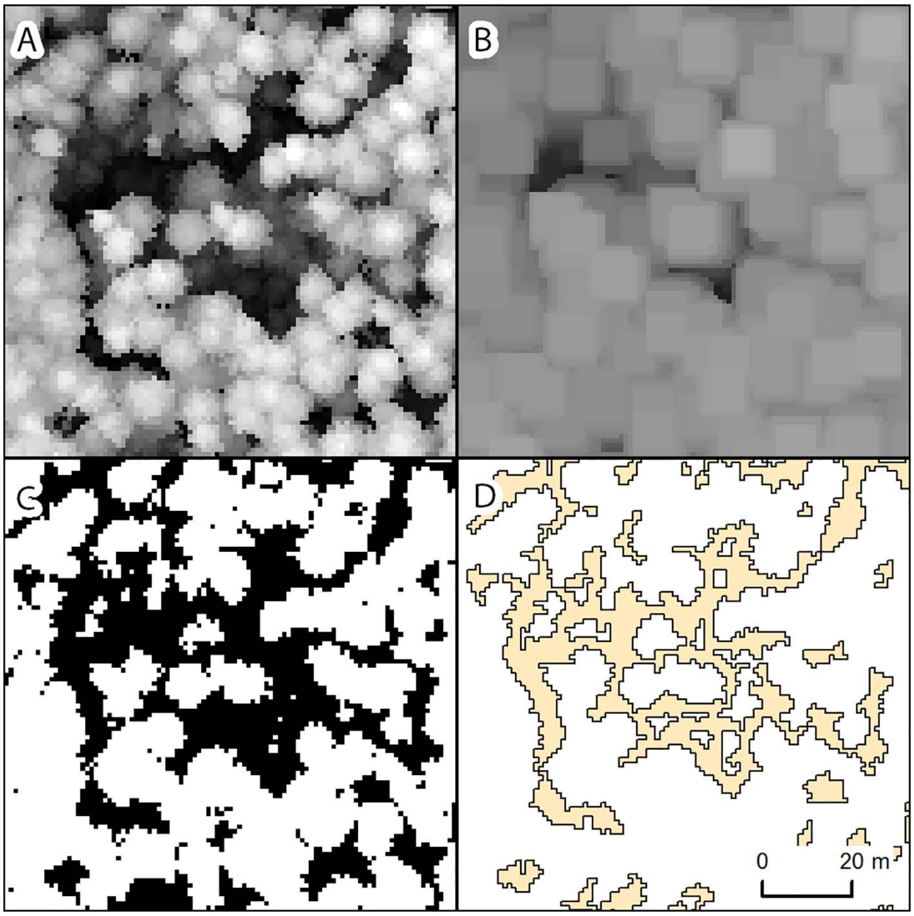

Fig. 2. Methodology for the variable-height threshold approach to canopy gap detection. First, a moving window (11 × 11 pixels in size) was applied to the canopy height model (CHM; A) to identify the top of the canopy (B). A height threshold raster was generated by calculating 64% of the top of canopy raster. For each CHM pixel, the difference between the CHM value and the height threshold raster value was calculated (C). Negative values shown as black, and positive as white. A pixel was identified as a gap if the difference (C) was < 64% of the corresponding maximum height.

detected gaps for the ROI as a whole, as well as relative to the flight lines used for the digital image acquisition. We established a buffer relative to the acquisition flight lines, within which view angles for acquisition were close to nadir (± 5°). We then compared the amount of overlap between the ALS and DAP gaps for both the fixed and variable threshold approaches within and external to this buffer. We also examined the distribution of gaps within each of the different seral stages in the ROI (Table 2).

2.5. Validation of gap detection

Validation data were derived using visual image interpretation. Outputs generated using the fixed- and variable-height threshold approaches were validated independently. For the fixed-height threshold approach, the analysis area was stratified into "gap" and "not gap" strata. The "gap" stratum was defined by combining gaps detected using the fixed-height threshold approach on both the ALS and DAP data. The "no gap" stratum was defined as the inverse of the gap stratum. A random sample of 100 points was generated for each stratum for a total of 200 samples. The interpreter was given the CHM_{ALS} and the 1 m orthophoto data to support their interpretation of "gap" or "not gap" for each reference point according to the fixed-threshold criteria (i.e. canopy height < 3 m, and gap size > 5 m^2 and < 2 ha). To ensure independence, the interpreter was not aware of which stratum the sample points were derived from, nor was the interpreter given access to the ALS or DAP detected gaps. Upon inspection, the interpreter assigned each sample as either "gap" (n = 87) or "not gap" (n = 113).

The same validation process was applied to the outputs generated with the variable-height threshold approach, with the gap stratum generated from the combined outputs of the variable-height threshold approach applied to the ALS and DAP data (and the "not gap" stratum being the inverse). A separate sample of 100 points was generated from each stratum and the interpreter inspected each point using the CHM_{ALS} and the 1 m orthophoto. An additional variable height raster, representing the height threshold value for the gap detection was generated to aid the interpreter in correctly identifying gaps. Once again, the interpreter was not aware of which stratum the sample points were derived from, nor was the interpreter given access to the ALS or DAP detected gaps. Each reference point was evaluated against the variable-height threshold criteria (i.e. canopy height < 64% of the average height in an 11 × 11 window, gaps size > 5 m^2 and < 2 ha) and was assigned as either "gap" (n = 105) or "not gap" (n = 95).

2.6. Generation of gap characteristics

Gap size distribution can inform on landscape-level characteristics (Asner et al., 2013). The gap size-frequency distribution provides a summary of the frequency with which gaps of a certain size occur, and is characterized by the exponent (λ) of a power-law probability density, the Zeta distribution (also referred to as the discrete Pareto distribution; Johnson et al., 2005, White et al., 2008). As demonstrated by Kellner and Asner (2009) the power-law Zeta distribution is suitable for characterizing the distribution of gap area. The λ value represents the negative slope between gap area and the frequency of gaps when plotted on a log-log scale. Values of λ are larger when the slope is steeper (i.e. when there are more small gaps; Kellner and Asner, 2009), and are expected to range from 1.0 to 3.0 in forest environments, with a threshold of 2.0 used to distinguish whether a forest is dominated by small (i.e. λ > 2.0) or large gaps (i.e. λ < 2.0) (Asner et al., 2013). We were interested in the differences of the λ-value when calculated for gaps generated using different input data (CHM_{ALS} and CHM_{DAP}) and different approaches to detect canopy gaps (fixed and variable height thresholds). We derived the λ parameter for the Zeta distribution using a maximum likelihood estimator, following the method described in Hanel et al. (2017). To determine whether or not our gap size distributions were sampled from a power-law distribution, we implemented the two-sided Kolmogorov-Smirnov test according the approach described in Hanel et al. (2017).

In addition to the gap size frequency distribution, a number of other characteristics were calculated to describe gap size, shape, and canopy properties inside a detected gap. A shape index (McGarigal and Marks, 1994) was used to characterize the complexity of a gap boundary. The shape index was calculated as a normalized ratio of gap perimeter to its area:

$$shape\ index = \frac{perimeter}{2*(\pi*area)^{0.5}}$$

The shape index of a perfectly circular gap will have a value of 1. The more complex the shape of the gap boundary, the higher value of the shape index. Distance to nearest gap was used to inform on the gap density in the study area and was calculated as the lowest value between the bounding box of a particular gap and the bounding boxes of gaps in its neighbourhood. CHM pixels within each gap were used to calculate mean canopy height and standard deviation of canopy height, for each data type, resulting in four statistics describing the canopy height inside a detected gap: mean height of CHM_{ALS} (H_{ALS}), mean height of CHM_{DAP} (H_{DAP}), standard deviation of CHM_{ALS} (SD_{ALS}), and standard deviation of CHM_{DAP} (SD_{CHM}).

3. Results

3.1. Comparison of ALS and DAP CHMs

We compared the derived canopy height models to determine the relative quality of CHM_{DAP} in our analysis area (Table 5 and Fig. 3). Overall, 62% of pixels within the CHM_{DAP} were within ± 5 m of the CHM_{ALS} canopy heights. The degree of similarity between CHM_{DAP} and CHM_{ALS} varied by seral stage, with old seral stage forests having the lowest correlation (r = 0.75) and the highest RMSE (9.41 m).

3.2. Gap detection and validation results

The total number of gaps detected with ALS and DAP data varied markedly, for both the fixed- and variable-height threshold approaches (Fig. 4), with the ALS data resulting in a greater number of gaps for both height threshold approaches (Table 6).

When the fixed-threshold approach was applied to the ALS data, we identified 6.5 times more total gap area compared to when the same approach was applied to the DAP data (Table 6). The average ALS gap size was 2 times smaller than the average DAP gap size, and the DAP data had markedly greater variability in gap size (standard deviation = 418.23 m^2) compared to the gaps identified with the ALS data (standard deviation = 142.66 m^2). In contrast to the fixed variable approach, the mean gap size for the variable threshold approach was larger for the ALS data (61.22 m^2) compared to the DAP data (25.37 m^2). The proportion of the ROI identified as gap with the DAP data and the variable threshold approach was 3.13%, which was similar to the result achieved using the ALS data and the fixed-height threshold approach (3.47%).

We evaluated the degree of overlap between the DAP- and ALS-detected gaps (Table 7) for the ROI as a whole, as well as relative to the flight lines used for the DAP acquisition. In the ROI, the median proportion of overlap between DAP and ALS gaps detected with the fixed threshold was 33.53% (mean = 42.90%), compared to a median of 3.84% (mean = 13.26%) for the gaps detected with the variable threshold. Trends in the proportion of DAP gaps that overlapped with ALS gaps in the ROI were consistent within and external to the near-nadir buffer, for both the fixed and variable threshold approach. Overall, although markedly more gaps were detected with variable threshold approach for both data sources, this increase in the number of detected gaps did not result in a concomitant increase in spatial overlap between the detected gaps.

We also investigated the distribution of detected gaps relative to seral stage and found that 71% of gaps detected with the ALS data using the fixed-threshold approach were found in old seral stage forests, whereas 65% of gaps derived from DAP data were found in early seral stage forests (Fig. 5). In old seral stage forests, the proportion of gaps detected with the variable threshold approach were twice that detected using the fixed threshold approach.

The overall accuracies of gaps identified using CHM_{ALS} were 96.50% and 89.50% for the fixed- and variable-height threshold approaches, respectively (Table 8). This compares to overall accuracies of 59.50% and 50.00% achieved using CHM_{DAP} data. While errors of omission and commission are relatively balanced for the ALS detected gaps, the gaps detected with the DAP data had larger errors of omission exceeding 88% for both approaches, as well as large errors of commission (> 40%) for areas that were not gap. The variable-height threshold approach resulted in an increase in omission error of 11.39% for the ALS data.

For the fixed-threshold approach, we also evaluated the relative gap detection accuracy in the early and old seral stages (Table 9). For the DAP data, overall accuracy for gap detection in early seral stage forests was 80%, compared to 50% in old seral stage forests. Likewise, accuracy of gap detection for the ALS data was 100.00% in the early seral stage forests, with larger omission errors for gaps (9.80%) in old seral stage forests.

3.3. Gap characteristics

The gaps generated using both data sources and both approaches were characterized using a number of different metrics in addition to the size and area metrics reported in Table 6. Average canopy heights within the detected gaps further corroborated the low level of spatial coincidence for gaps detected with ALS and DAP (Table 10). Mean canopy heights from the ALS and DAP data within ALS-identified gaps were significantly different (*t*-test; $p < 0.05$). The mean H_{DAP} was 26.15 m, compared to a mean H_{ALS} of 1.59 m, indicating that much of the area identified as gap using the ALS data was not identified as gap using the DAP data. Differences between mean canopy heights for H_{DAP} and H_{ALS} were less pronounced in gaps identified using the DAP data:

Table 5
Summary measures of comparison of DAP CHM to ALS CHM.

Metric	ROI	Seral stage			
		< 40 years	40–80 years	80–250 years	> 250 years
Pearson's r	0.88	0.89	0.96	0.83	0.75
RMSE (m)	7.88	3.69	5.04	7.17	9.41
RMSE (%)	29.80	23.26	18.67	21.59	34.07
Percentage of DAP pixels within ± 5 m of ALS heights (%)	62	83	72	64	51
Percentage of DAP pixels within ± 10 m of ALS heights (%)	95	98	94	88	77

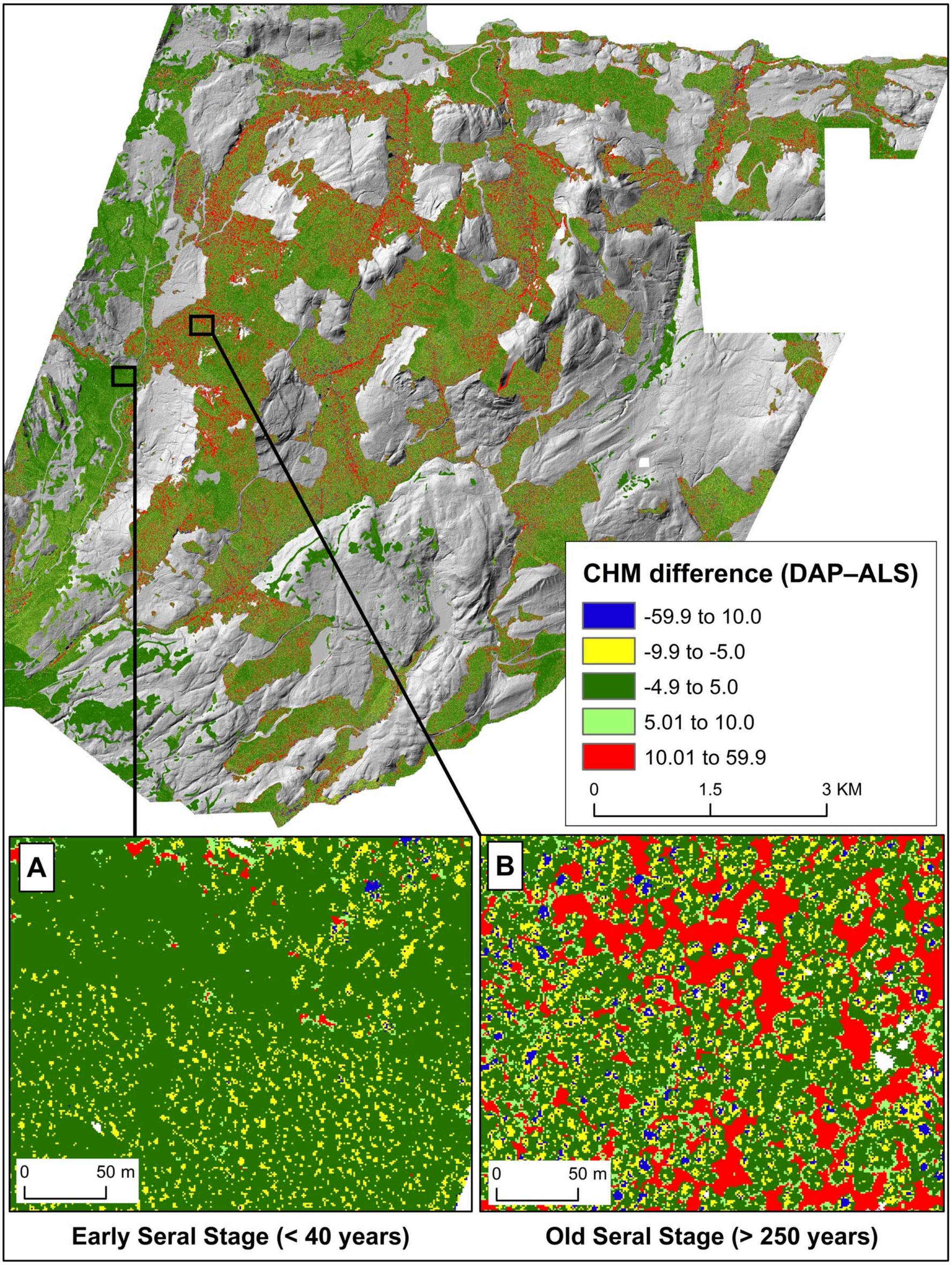

Fig. 3. Wall-to-wall comparison of DAP and ALS CHMs. Insets show differences between the two CHMs for (A) early seral stage forests and (B) old seral stage forests.

mean H_{DAP} was 1.55 m compared to a mean H_{ALS} of 4.96 m. Differences between mean values of H_{ALS} and H_{DAP} in gaps detected using the variable threshold approach were not as large as for the fixed-height threshold approach (Fig. 6).

In examining the distribution of gap sizes, we found that canopy gap size frequency distributions followed a power-law Zeta distribution for both data types and approaches (Fig. 7; Table 11). For the fixed-height threshold approach, $\lambda = 1.85$ for ALS-derived gaps and $\lambda = 1.67$ for DAP-derived gaps, corroborating the greater frequency of smaller gaps detected with the ALS data (Table 6). Conversely, for the variable-height threshold approach, values of λ were larger for the DAP-derived gaps ($\lambda = 2.04$), relative to the ALS-derived gaps ($\lambda = 1.70$), which also corresponds to the smaller average gap size associated with the DAP data for the variable threshold approach (Table 6).

On average, distance-to nearest gap was 13.67 m and 10.16 m for the ALS derived gaps compared to 34.42 m and 11.30 m for the DAP-

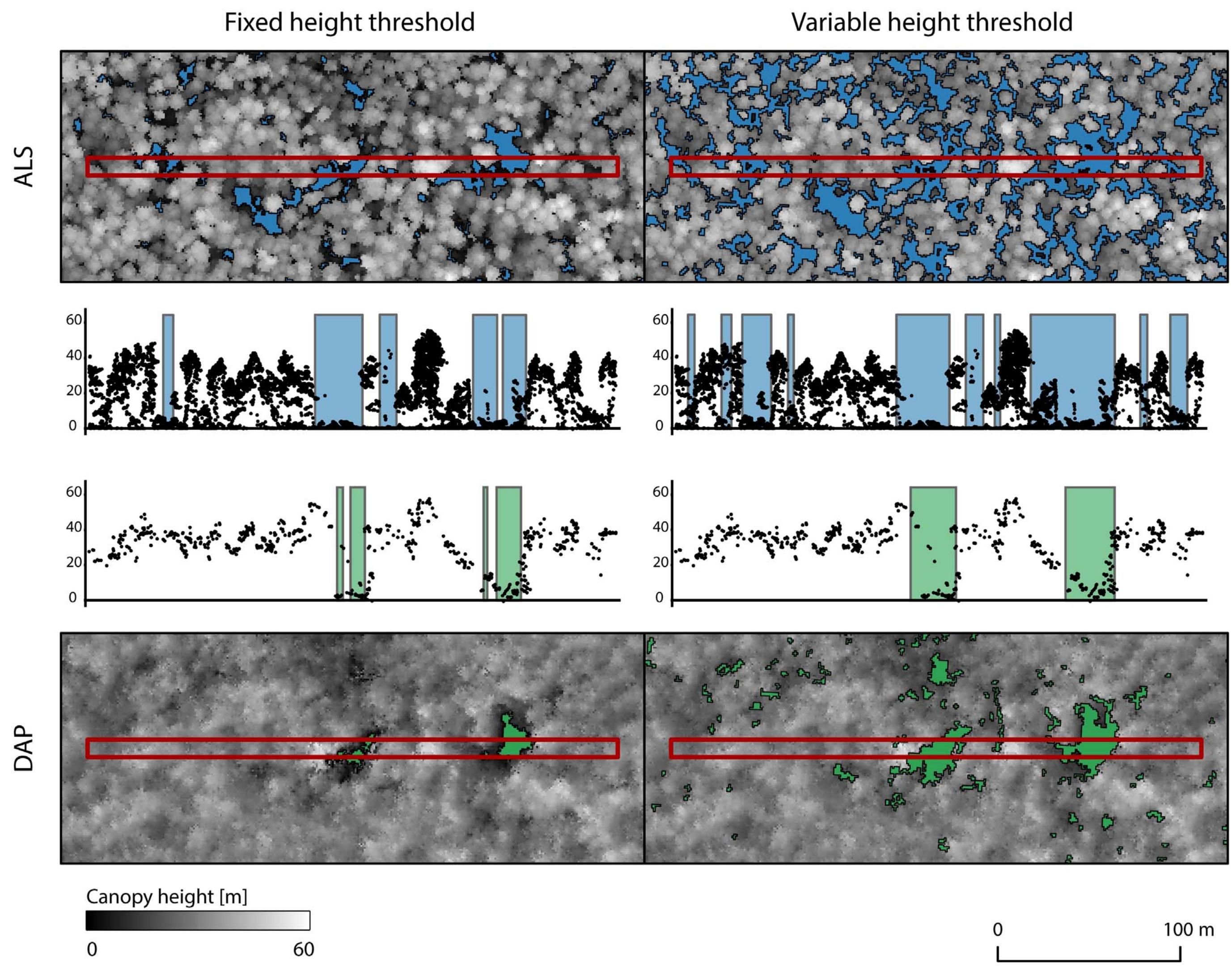

Fig. 4. Results of canopy gap detection using a fixed or variable height threshold.

Table 6
Summary statistics for canopy gaps detected using CHM_{ALS} and CHM_{DAP}.

Data source	Number of gaps	Total area of gaps (ha)	Proportion of ROI that is gap	Mean gap size (m^2)	Median gap size (m^2)	SD gap size (m^2)
Fixed-height threshold approach						
ALS	52,085	151.09	3.47%	29.01	11.00	142.66
DAP	3149	23.25	0.54%	56.48	12.00	418.23
Variable-height threshold approach						
ALS	127,972	783.47	18.03%	61.22	13.00	462.54
DAP	53,590	135.93	3.13%	25.37	9.00	159.92

derived gaps when using a fixed and variable-height threshold approach, respectively (Fig. 6). Average shape index values were consistently between 1.5 and 1.7 for both data sources and approaches, with more similarity in shape index values between the gaps identified using ALS and DAP data when the variable-height threshold approach was applied.

4. Discussion

Prior to this study, the relative capacity of DAP data for canopy gap mapping and characterization had not been investigated and compared to that of ALS data. Our results indicate significant differences in the number and size of gaps detected using ALS and DAP data, as well as large differences in the accuracy of gap detection. ALS data identified markedly more gaps and gap area, whether using the fixed- or the variable-height threshold approaches (Table 6), and there were large errors of omission (> 80%) in gap detection when using DAP data with either approach (Table 8). We attribute these differences to the characteristics of the DAP data itself and the complexity of the forest environment. DAP data primarily characterize the outer canopy envelope (Fig. 4; White et al., 2013) and shadows and occlusions from surrounding trees can negatively impact image matching, particularly in the stereo-matching scenario applied in this study, which thereby impairs the detection of small canopy gaps (Vastaranta et al., 2013).

A variety of different data sources have been investigated for mapping canopy gaps, including very high spatial resolution stereo satellite images (WorldView-2; Hobi et al., 2015) and terrestrial laser scanning data (Siedl et al., 2015). ALS data has been used extensively for mapping canopy gaps, across a range of forest environments (Table 1). Zielewska-Büettner et al. (2016) mapped forest gaps in 2009 and 2012 for a 1023-ha forest are in southern Germany using DAP data. The authors used similar imagery to what was applied in this study (UltraCamXP imagery with a 20 cm GSD, 60% along-track overlap, and 30% across-track overlap), from which they generated a 1-m CHM and applied fixed height thresholds of 1 m and 2 m to identify canopy gaps

Table 7
Summary of overlap characteristics between DAP- and ALS-detected gaps within our region of interest (ROI) overall, and within a spatial buffer defined relative to image acquisition flight lines (representing view angles ± 5°), and external to this buffer.

	ROI	Within buffer (± 5° from nadir)	External to buffer
Fixed threshold for gap detection			
Total number of ALS gaps	52,085	14,056	38,029
Total number of DAP gaps	3149	1018	2131
Total number of DAP gaps with some degree of overlap with ALS gaps	2077	676	1401
% of DAP gaps overlapping with ALS gaps	65.96	66.40	65.74
Amount of overlap (%)			
Mean	42.90	39.08	44.91
Median	33.53	30.00	37.01
Standard deviation	36.17	35.02	36.61
Minimum	0.03	0.03	0.03
Maximum	100.00	100.00	100.00
Variable threshold for gap detection			
Total number of ALS gaps	127,972	30,192	97,780
Total number of DAP gaps	53,590	16,130	37,460
Total number of DAP gaps with some degree of overlap with ALS gaps	42,378	11,271	26,826
% of DAP gaps overlapping with ALS gaps	79.08	69.88	71.61
Amount of overlap (%):			
Mean	13.26	13.10	13.33
Median	3.84	3.49	4.00
Standard deviation	19.89	19.71	19.97
Minimum	0.01	0.01	0.01
Maximum	100.00	100.00	100.00

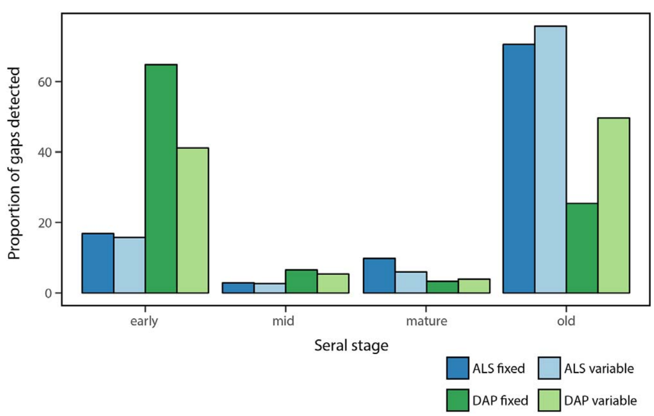

Fig. 5. Results of canopy gap detection using a fixed or variable height threshold, by seral stage.

Table 8
Gap detection validation results.

	Overall accuracy	Gap		Not gap	
		Omission error	Commission error	Omission error	Commission error
Fixed-height threshold approach					
ALS	96.50%	5.75%	2.38%	1.77%	4.31%
DAP	59.50%	90.80%	20.00%	1.77%	41.58%
Variable-height threshold approach					
ALS	89.50%	17.14%	3.33%	3.16%	16.36%
DAP	50.00%	88.57%	36.84%	7.37%	51.38%

in low (< 8 m) and high (≥8 m) forests, respectively. The authors used visual-stereo interpretation for validation, and commensurate with our findings, reported large omission errors in gap detection in 2009 (30%) and 2012 (48%) in forests that were ≥8 m in height (Zielewska-Büettner et al., 2017). The authors attributed these errors to the increased prevalence of shadows and occlusions in tall forests. In our study, overall accuracy for gap detection for the DAP data (fixed-height threshold) was 80% in early seral stages (ALS mean height = 15.8 m)

Table 9
Accuracy of gap detection using the fixed-threshold approach in early and old seral stage forests.

	Overall accuracy	Gap		Not gap	
		Omission error	Commission error	Omission error	Commission error
Early seral stage (n = 30)					
ALS	100.00%	0.00%	0.00%	0.00%	0.00%
DAP	80.00%	50.00%	16.67%	5.01%	20.83%
Old seral stage (n = 98)					
ALS	93.88%	9.80%	2.13%	2.13%	9.80%
DAP	50.00%	96.08%	0.00%	0.00%	51.01%

Table 10
Summary of canopy heights within identified gaps.

Data source	Mean of H_{ALS} (m)	SD of H_{ALS} (m)	Mean of H_{DAP} (m)	SD of H_{DAP} (m)
Fixed-height threshold				
ALS	1.59	0.57	26.15	9.98
DAP	4.96	5.41	1.55	0.71
Variable-height threshold				
ALS	14.51	6.02	24.25	9.79
DAP	17.37	9.02	13.95	5.93

compared to 50% in old seral stages (ALS mean height = 27.6 m), whereas the accuracy of gap detection with the ALS data varied by only ~6% between early and old seral stages. Old seral stage forests in this study area contain larger trees (the mean ALS canopy height was 27.58 m in old seral stage forests compared to 15.80 in early seral stage forests; Table 2), and are characterized by increased shadows and occlusions.

The gap size frequency distribution used in this study provides a useful, single metric for comparative purposes within and among different forest ecosystems (e.g. Andrew et al., 2016). Gap size influences factors such as light intensity and soil moisture, which in turn influences regeneration effectiveness (Muscolo et al., 2014) and growth response (Stan and Daniels, 2014). Studies that have reported gap size frequency distributions have been conducted in tropical forests (e.g.

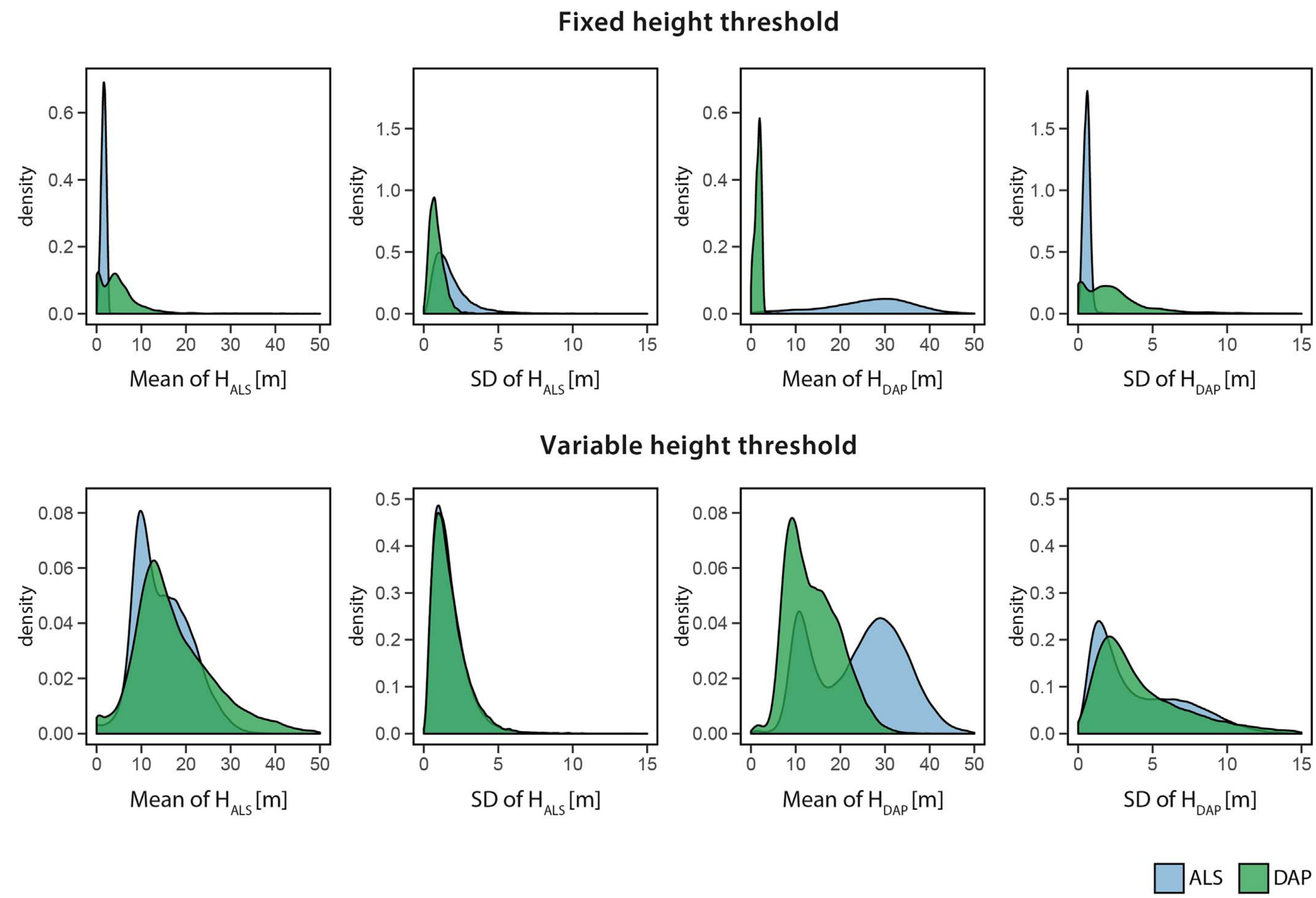

Fig. 6. Height characteristics for gaps detected using ALS and DAP with fixed- and variable-height thresholds.

Fisher et al., 2008; Lloyd et al., 2009; Kellner and Asner, 2009; Boyd et al., 2013; Asner et al., 2013) and to our knowledge, there has been no research that compares the scaling parameters derived in tropical forests to those in temperate or boreal forests. Lobo and Dalling (2014) demonstrated that the height thresholds used in gap definition have an impact on λ-values, and this effect is also evident in our results when we compare the scaling parameters from gaps generated from the same data source, but with a fixed- or variable-height threshold (e.g. DAP $\lambda = 1.67$ for fixed threshold and $\lambda = 2.04$ for variable threshold).

In contrast to other studies that have demonstrated a similar performance between ALS and DAP data for area-based forest inventory estimation (e.g. Vastaranta et al., 2013; Stepper et al., 2014; White et al., 2015), for this application, the DAP data failed to detect and map gaps with the same level of accuracy as the ALS data, regardless of whether fixed- or variable-height thresholds were applied. It should be noted that our validation approach assesses the capacity of ALS and DAP to detect the presence or absence of a gap, and does not inform on the degree to which these data sources accurately characterize gap size or shape. We have however assessed the amount of overlap between the DAP and ALS detected gaps in order to get a relative sense of the similarity in area for individual gaps (Table 7). Moreover, we noted no difference in gap overlap as a function of image acquisition view angles.

Carefully constructed image-based point clouds derived from DAP data can reliably characterize dominant canopy heights, which is a key predictor that drives the area-based approach for estimating forest inventory attributes of interest such as dominant height or volume (White et al., 2013). However, our results indicate that stereo-image matching does not consistently capture small canopy openings, which are critical for accurate gap detection. Similar limitations for DAP data are identified in Ali-Sisto and Packalén (2017), who reported that DAP data performed poorly in the detection of minor forest changes. Vehmas et al. (2011) used ALS data to detect and map gaps in boreal forests, and then used gap characteristics to distinguish between semi-natural and managed forests. In their application, the authors found that the most useful metrics for discriminating between semi-natural and managed forests were related to the vertical distribution of low vegetation within the identified gaps. Based on the results of our study and earlier work with DAP data in this forest type (White et al., 2015), we conclude that DAP data would not be capable of supporting this form of detailed within-gap analysis of vegetation. It should be noted that our results and those of Zielewska-Büettner et al. (2016, 2017) convey the capacity of DAP data derived from stereo matching, which is currently the most common form of DAP data being used in forest applications. As noted earlier, Hirschmugl et al. (2007) demonstrated the potential of multi-image matching (enabled by greater forward image overlap) for gap mapping, indicating a need for further research on the capacity of DAP data derived from multi-image matching for this application.

As noted by Gobakken et al. (2014) investment decisions in 3D data to support forest management must consider not only the costs of data acquisition and processing, but also the full value of the information to support decision making. The results of this study demonstrate some important differences between ALS and stereo DAP data for detecting and characterizing canopy gaps. These differences have implications for gap surveys and for monitoring of gap dynamics over time and suggest that, given the DAP data currently in widespread use, ALS data would be the data source of choice for this application, particularly in coastal temperate rainforests with complex canopy architecture.

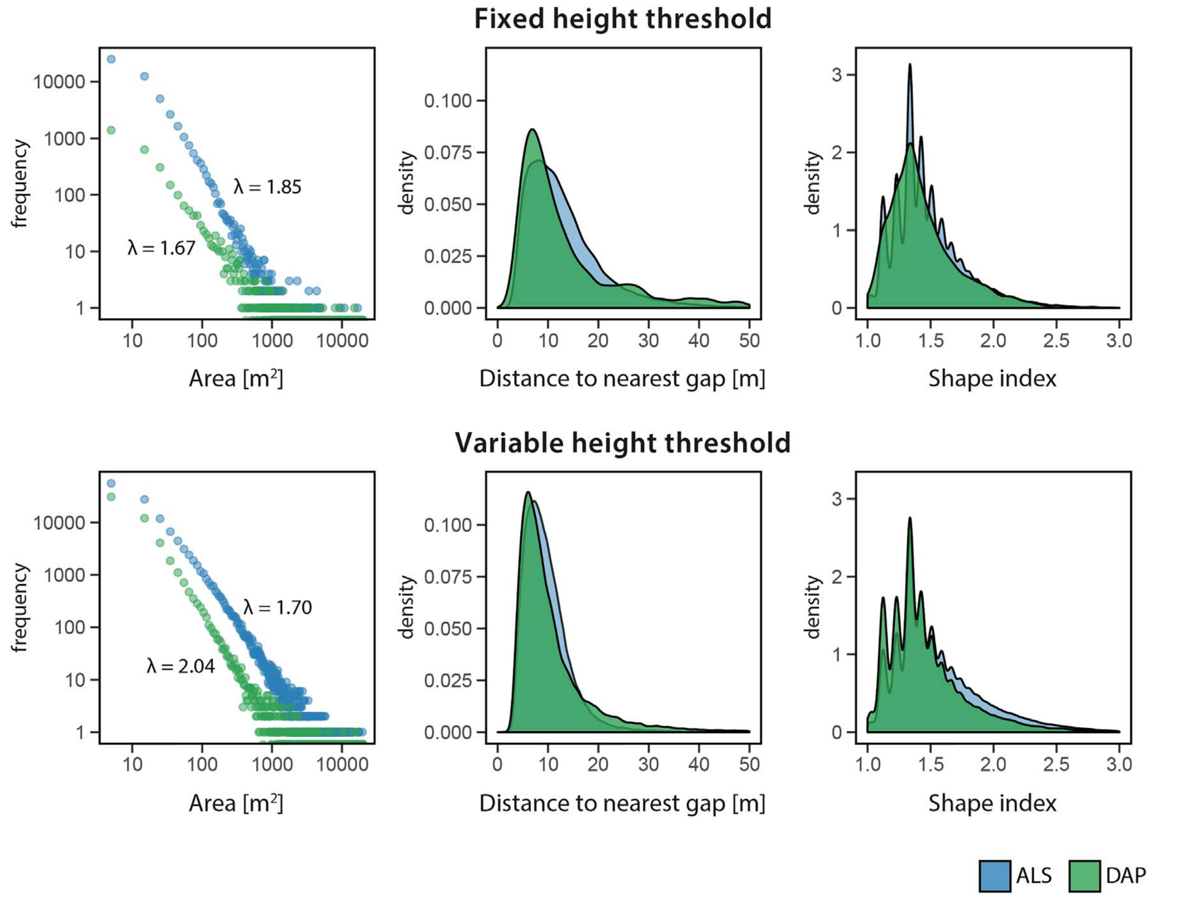

Fig. 7. Gap size frequency distribution, distance to nearest gap, and gap shape index using the fixed- and variable-height threshold approaches for gap detection.

Table 11
Results of the two-sided Kolmogorov-Smirnov goodness of fit test (α = 0.05).

Data	λ	Sample size	KS (critical value)	KS (D)
Fixed height threshold				
ALS	1.8463	52,085	0.9863	0.0322
DAP	1.6707	3149	0.9673	0.0161
Variable height threshold				
ALS	1.7039	127,972	0.9862	0.0227
DAP	2.0462	53,590	0.9942	0.0202

5. Conclusions

Based on the results of this study in a complex coastal temperate forest, DAP data generated via stereo-matching did not provide detailed and accurate maps of canopy gaps that were analogous to results achieved using ALS data with either the fixed- or variable-height threshold approaches. Marked differences in the number and size of canopy gaps identified using ALS and DAP data, their lack of spatial correspondence, and the concentration of the DAP-derived gaps in early seral stages suggest that DAP data are not capable of characterizing small canopy openings and are confounded by the increased prevalence of shadows and occlusions found in mature and old seral stage forest canopies. Variable-height threshold approaches resulted in lower accuracies for both ALS and DAP data and, as they are more computationally intensive to implement, they are not advantageous unless there is a specific information need related to characterizing gaps in the upper canopy. ALS data provided a detailed and accurate characterization of canopy gaps in this coastal temperate forest with a fixed-height threshold approach. With the ALS data, the accuracy of the approach did not vary by seral stage and was robust across the range of stand conditions present in the study area. Future research should explore further the characteristics of the presented approach to gap size frequency distributions in temperate and boreal forest environments.

Acknowledgements

This research was supported by the Canadian Wood Fibre Centre (CWFC) of the Canadian Forest Service, Natural Resources Canada. Western Forest Products Inc. is thanked for sharing the data used in this research. We also thank Christoph Stepper for processing the image data, and Mathias Schardt and Karl-Heinz Gutjahr from Joanneum Research, Graz, for assistance with the RSG software. Support was also provided by a Natural Sciences and Engineering Research Council of Canada (NSERC, RGPIN 311926-13) grant to Nicholas Coops. We thank the editors and two anonymous reviewers for their time and efforts.

References

Aldred, A., Bonner, M., 1985. Application of airborne lasers to forest surveys. In: Canadian Forestry Service, Petawawa National Forestry Centre, Information Report PI-X-51, Available online. http://cfs.nrcan.gc.ca/pubwarehouse/pdfs/4525.pdf, Accessed date: 1 April 2017 (62 pp).
Ali-Sisto, D., Packalén, P., 2017. Forest change detection by using point clouds from dense image matching together with a LiDAR-derived terrain model. IEEE J. Sel. Top. Appl. Earth Obs. Remote Sens. 10 (3), 1197–1206.
Andersen, H.E., Reutebuch, S.E., McGaughey, R.J., 2006. A rigorous assessment of tree height measurements obtained using airborne LiDAR and conventional field methods. Can. J. Remote. Sens. 32, 355–366.
Andrew, M.E., Ruthrof, K., Matusick, G., St. J. Hardy, G.E., 2016. Spatial configuration of drought disturbances and forest gap creation across environmental gradients. PLoS One 11 (6).
Asner, G.P., Kellner, J.R., Kennedy-Bowdoin, T., Knapp, D.E., Anderson, C., Martin, R.E., 2013. Forest canopy gap distributions in the southern Peruvian Amazon. PLoS One 8 (4).
Axelsson, P., 2000. DEM generation from laser scanner data using adaptive TIN models. P.

110–117 in International Archives of Photogrammetry and Remote Sensing XXXIII. In: International Society for Photogrammetry and Remote Sensing. Amsterdam, The Netherlands.
B.C. Ministry of Forests, B.C. Ministry of Environment, Lands and Parks, 1997. Biodiversity guidebook. Available online. https://www.for.gov.bc.ca/hfd/library/documents/bib19715.pdf, Accessed date: 27 April 2017 (Victoria, BC).
Baltsavias, E.P., 1999. A comparison between photogrammetry and laser scanning. ISPRS J. Photogramm. Remote Sens. 54, 83–94.
Baltsavias, E.P., Gruen, A., Eisenbeiss, H., Zhang, L., Waser, L.T., 2008. High-quality image matching and automated generation of 3D tree models. Int. J. Remote Sens. 29 (5), 1243–1259.
Bohlin, J., Wallerman, J., Fransson, J.E.S., 2012. Forest variable estimation using photogrammetric matching of digital aerial images in combination with high-resolution DEM. Scand. J. For. Res. 27, 692–699.
Bohlin, J., Bohlin, I., Jonzén, J., Nilsson, M., 2017. Mapping forest attributes using data from stereophotogrammetry of aerial images and field data from the national forest inventory. Silva Fennica 51 (2), 1–18.
Bonnet, S., Gaulton, R., Lehaire, F., Lejeune, P., 2015. Canopy gap mapping from airborne laser scanning: an assessment of the positional and geometrical accuracy. Remote Sens. 7 (9), 11267–11294.
Boyd, D.S., Hill, R.A., Hopkinson, C., Baker, T.R., 2013. Landscape-scale forest disturbance regimes in southern Peruvian Amazonia. Ecol. Appl. 23 (7), 1588–1602.
Burton, P., Parisien, M.-A., Hicke, J.A., Hall, R.J., Freeburn, J.T., 2008. Large fires as agents of ecological diversity in North American boreal forest. Int. J. Wildland Fire 17 (6), 754–767.
Daniels, L.D., Gray, R.W., 2006. Disturbance regimes in coastal British Columbia. Br. Columbia J. Ecosyst. Manage. 7 (2), 44–56.
de Lima, R.A.F., 2005. Gap size measurement: the proposal of a new field method. For. Ecol. Manag. 214, 413–419.
Fisher, J.I., Hurtt, G.C., Thomas, R.Q., Chambers, J.Q., 2008. Clustered disturbances lead to bias in large-scale estimates based on forest sample plots. Ecol. Lett. 11, 554–563.
Fox, T.J., Knutson, M.G., Hines, R.K., 2000. Mapping forest canopy gaps using air-photo interpretation and ground surveys. Wildl. Soc. Bull. 28 (4), 882–889.
Gaulton, R., Malthus, T.J., 2010. LiDAR mapping of canopy gaps in continuous cover forests: a comparison of canopy height model and point cloud based techniques. Int. J. Remote Sens. 31 (5), 1193–1211.
Gobakken, T., Bollandsås, O.M., Næsset, E., 2014. Comparing biophysical forest characteristics estimated from photogrammetric matching of aerial images and airborne laser scanning data. Scand. J. For. Res. 30, 73–86.
Granholm, A.-H., Lindgren, N., Olofsson, K., Nyström, M., Allard, A., Olsson, H., 2017. Estimating vertical canopy cover using dense image-based point cloud data in four vegetation types in southern Sweden. Int. J. Remote Sens. 38 (7), 1820–1838.
Gray, A.N., Spies, T.A., 1996. Gap size, within-gap position and canopy structure effects on conifer seedling establishment. J. Ecol. 84, 635–645.
Gray, A.N., Spies, T.A., Pabst, R.J., 2012. Canopy gaps affect long-term patterns of tree growth and mortality in mature and old-growth forests in the Pacific Northwest. For. Ecol. Manag. 281, 111–120.
Gruen, A., 2012. Development and status of image matching in photogrammetry. Photogramm. Rec. 27 (137), 36–57.
Hanel, R., Corominas-Murtra, B., Liu, B., Thurner, S., 2017. Fitting power-laws in empirical data with estimators that work for all exponents. PLoS One 12 (2), e0170920.
Harestad, A.S., 1985. Habitat use by black-tailed deer on northern Vancouver Island. J. Wildl. Manag. 49 (4), 946–950.
Hawryło, P., Tompalski, P., Wężyk, P., 2017. Area-based estimation of growing stock volume in Scots pine stands using ALS and airborne image-based point clouds. Forestry i, 1–11. http://dx.doi.org/10.1093/forestry/cpx026.
Hirschmugl, M., Ofner, M., Raggam, J., Schardt, M., 2007. Single tree detection in very high resolution remote sensing data. Remote Sens. Environ. 110, 533–544.
Hirschmüller, H., 2008. Stereo processing by semiglobal matching and mutual information. IEEE Trans. Pattern Anal. Mach. Intell. 30, 328–341.
Hobi, M.L., Ginzler, C., Commarmot, B., Bugmann, H., 2015. Gap pattern of the largest primeval beech forest of Europe revealed by remote sensing. Ecosphere 6 (5), 1–21.
Honkavaara, E., Markelin, L., Rosnell, T., Nurminen, K., 2012. Influence of solar elevation in radiometric and geometric performance of multispectral photogrammetry. ISPRS J. Photogramm. Remote Sens. 67, 13–26.
Järnstedt, J., Pekkarinen, A., Tuominen, S., Ginzler, C., Holopainen, M., Viitala, R., 2012. Forest variable estimation using a high-resolution digital surface model. ISPRS J. Photogramm. Remote Sens. 74, 78–84.
Johnson, N.L., Kemp, A.W., Kotz, S., 2005. Univariate Discrete Distributions, third edition. Wiley-Interscience, New York, New York, USA.
Kane, V.R., Gersonde, R.F., Lutz, J.A., McGaughey, R.J., Bakker, J.D., Franklin, J.F., 2011. Patch dynamics and the development of structural and spatial heterogeneity in Pacific Northwest forests. Can. J. For. Res. 41, 2276–2291.
Kellner, J.R., Asner, G.P., 2009. Convergent structural responses of tropical forests to diverse disturbance regimes. Ecol. Lett. 12, 887–897.
Kukkonen, M., Maltamo, M., Packalen, P., 2017. Image matching as a data source for forest inventory – comparison of Semi-Global Matching and Next-Generation Automatic Terrain Extraction algorithms in a typical managed boreal forest environment. Int. J. Appl. Earth Obs. Geoinf. 60, 11–21.
Leberl, F., Irschara, A., Pock, T., Meixner, P., Gruber, M., Scholz, S., Wiechert, A., 2010. Point clouds: LiDAR versus 3D vision. Photogramm. Eng. Remote. Sens. 76, 1123–1134.
Lefsky, M.A., Cohen, W.B., Acker, S.A., Parker, G.G., Spies, T.A., Harding, D., 1999. Lidar remote sensing of the canopy structure and biophysical properties of Douglas-fir western hemlock forests. Remote Sens. Environ. 70, 339–361.
Lertzman, K.P., Sutherland, G.D., Inselberg, A., Saunders, S.C., 1996. Canopy gaps and the landscape mosaic in a coastal temperate rain forest. Ecology 77 (4), 1254–1270.
Lertzman, K., Spies, T., Swanson, F., 1997. From ecosystem dynamics to ecosystem management. In: Schoonmaker, P.K., von Hagen, B., Wolf, E.C. (Eds.), The Rain Forests of Home: Profile of a North American Bioregion. Island Press, Covelo, Calif., pp. 361–382.
Lloyd, J., Gloor, E.U., Lewis, S.L., 2009. Are the dynamics of tropical forests dominated by large and rare disturbance events? Ecol. Lett. 12, E19–E21.
Lobo, E., Dalling, J.W., 2014. Spatial scale and sampling resolution affect measures of gap disturbance in a lowland tropical forest: implications for understanding forest regeneration and carbon storage. Proc. R. Soc. B 281, 20133218.
Massé, A., Côté, S.D., 2012. Linking habitat heterogeneity to space use by large herbivores at multiple scales: from habitat mosaics to forest canopy openings. For. Ecol. Manag. 285, 67–76.
McGarigal, K., Marks, B.J., 1994. FRAGSTATS: spatial pattern analysis program for quantifying landscape structure. In: General Technical Report PNW-GTR-351. U.S. Department of Agriculture, Forest Service, Pacific Northwest Research Station Available online. https://www.fs.fed.us/pnw/pubs/pnw_gtr351.pdf, Accessed date: 1 May 2017.
Meidinger, D.V., Pojar, J., 1991. Ecosystems of British Columbia. In: Special Report Series 6. British Columbia Ministry of Forests, Victoria, BC Available online. https://www.for.gov.bc.ca/hfd/pubs/Docs/Srs/Srs06.htm, Accessed date: 27 April 2017.
Muscolo, A., Bagnato, S., Sidari, M., Mercurio, R., 2014. A review of the roles of forest canopy gaps. J. For. Res. 25 (4), 725–736.
Næsset, E., 2002. Predicting forest stand characteristics with airborne scanning laser using a practical two-stage procedure and field data. Remote Sens. Environ. 80 (1), 88–99.
Næsset, E., 2015. Vertical height errors in digital terrain models derived from airborne laser scanner data in a boreal-alpine ecotone in Norway. Remote Sens. 7, 4702–4725.
Nelson, R., Krabill, W., Maclean, G., 1984. Determining forest canopy characteristics using airborne laser data. Remote Sens. Environ. 15, 201–212.
Nurminen, K., Karjalainen, M., Yu, X., Hyyppä, J., Honkavaara, E., 2013. Performance of dense digital surface models based on image matching in the estimation of plot-level forest variables. ISPRS J. Photogramm. Remote Sens. 83, 104–115.
Pitt, D.G., Woods, M., Penner, M., 2014. A comparison of point clouds derived from stereo imagery and airborne laser scanning for the area-based estimation of forest inventory attributes in boreal Ontario. Can. J. Remote. Sens. 40, 214–232.
Puliti, S., Gobakken, T., Ørka, H.O., Næsset, E., 2016. Assessing 3D point clouds from aerial photographs for species-specific forest inventories. Scand. J. For. Res. 32, 68–79.
Rahlf, J., Breidenbach, J., Solberg, S., Næsset, E., Astrup, R., 2017. Digital aerial photogrammetry can efficiently support large-area forest inventories in Norway. Forestry 90, 710–718.
Remondino, F., Spera, M.G., Nocerina, E., Menna, F., Nex, F., 2014. State of the art in high density image matching. Photogramm. Rec. 29 (146), 144–166.
Reutebuch, S.E., McGaughey, R.J., Andersen, H.-E., Carson, W.W., 2003. Accuracy of high-resolution LiDAR terrain model under a conifer forest canopy. Can. J. Remote. Sens. 29, 527–535.
Runkle, J.R., 1982. Patterns of disturbance in some old-growth mesic forests of eastern North America. Ecology 63 (5), 1533–1546.
Runkle, J.R., 1992. Guidelines and sample protocol for sampling forest gaps. In: United States Department of Agriculture, Forest Service, Pacific Northwest Research Station General Technical Report PNW-GTR-283, Available online. https://www.fs.fed.us/pnw/pubs/pnw_gtr283.pdf, Accessed date: 1 March 2017.
Safranyik, L., Carroll, A.L., Régnière, J., Langor, D.W., Riel, W., Shore, T.L., Peter, B., Cooke, B.J., Nealis, V.G., Taylor, S.W., 2010. Potential for range expansion of mountain pine beetle into the boreal forest of North America. Can. Entomol. 142, 415–422.
Schliemann, S.A., Bockheim, J.G., 2011. Methods for studying treefall gaps: a review. For. Ecol. Manag. 261, 1143–1151.
Siedl, D., Ammer, C., Puettmann, K., 2015. Describing forest canopy gaps efficiently, accurately, and objectively: new prospects through the use of terrestrial laser scanning. Agric. For. Meteorol. 213, 23–32.
Spies, T.A., Franklin, J.F., Thomas, T.B., 1988. Coarse woody debris in Douglas-fir forests of western Oregon and Washington. Ecology 69 (6), 1689–1702.
Stan, A.B., Daniels, L.D., 2010. Growth releases of three shade-tolerant species following canopy gap formation in old-growth forests. J. Veg. Sci. 21, 74–87.
Stan, A.B., Daniels, L.D., 2014. Growth releases across a natural canopy gap-forest gradient in old-growth forests. For. Ecol. Manag. 313, 98–103.
Stepper, C., Straub, C., Pretzsch, H., 2014. Using semi-global matching point clouds to estimate growing stock at the plot and stand levels: application for a broadleaf-dominated forest in central Europe. Can. J. For. Res. 45, 111–123.
St-Onge, B., Vega, C., Fournier, R.A., Hu, Y., 2008. Mapping canopy height using a combination of digital stereo-photogrammetry and lidar. Int. J. Remote Sens. 29 (11), 3343–3364.
St-Onge, B., Vepakomma, U., Sénécal, J-F., Kneeshaw, D., Doyon, F., 2014. Canopy gap detection and analysis with airborne laser scanning (Chapter 21) In: Maltamo, M., Næsset, E., Vauhkonen, J. (Eds.), Forestry Applications of Airborne Laser Scanning: Concepts and Case Studies. Springer, Dordrech. http://dx.doi.org/10.1007/978-94-017-8663-8. (464 pp).
Tahtinen, B., Murray, B.D., Webster, C.R., Tarasoff, C.S., Burton, A.J., 2014. Does ungulate foraging behavior in forest canopy gaps produce a spatial subsidy with cascading effects on vegetation? For. Sci. 60 (5), 819–829.
Ullah, S., Dees, M., Datta, P., Adler, P., Koch, B., 2017. Comparing airborne laser scanning, and image-based point clouds by semi-global matching and enhanced automatic terrain extraction to estimate forest timber volume. Forests 8, 1–15.
Vastaranta, M., Wulder, M.A., White, J.C., Pekkarinen, A., Tuominen, S., Ginzler, C.,

Kankare, V., Holopainen, M., Hyyppa, J., Hyyppa, H., 2013. Airborne laser scanning and digital stereo imagery measures of forest structure: comparative results and implications to forest mapping and inventory update. Can. J. Remote. Sens. 39, 382–395.
Vehmas, M., Packalén, P., Maltamo, M., Eerikäinen, K., 2011. Using airborne laser scanning data for detecting canopy gaps and their understory type in mature boreal forest. Ann. For. Sci. 68 (4), 825–833.
Vepakomma, U., St-Onge, B., Kneeshaw, D., 2008. Spatially explicit characterization of boreal forest gap dynamics using multi-temporal lidar data. Remote Sens. Environ. 112 (5), 2326–2340.
Vepakomma, U., St-Onge, B., Kneeshaw, D., 2011. Response of a boreal forest to canopy gap openings –assessing vertical and horizontal tree growth with multi-temporal lidar data. Ecol. Appl. 21 (1), 99–121.
Vepakomma, U., Kneeshaw, D., Fortin, M.J., 2012. Spatial contiguity and continuity of canopy gaps in mixed wood boreal forests: persistence, expansion, shrinkage and displacement. J. Ecol. 100 (5), 1257–1268.
White, E.P., Enquist, B.J., Green, J.L., 2008. On estimating the exponent of power-law frequency distributions. Ecology 89 (4), 905–912.
White, J.C., Wulder, M.A., Vastaranta, M., Coops, N.C., Pitt, D., Woods, M., 2013. The utility of image-based point clouds for forest inventory: a comparison with airborne laser scanning. Forests 4, 518–536.
White, J.C., Stepper, C., Tompalski, P., Coops, N.C., Wulder, M.A., 2015. Comparing ALS and image-based point cloud metrics and modelled forest inventory attributes in a complex coastal forest environment. Forests 6, 3704–3732.
White, J.C., Coops, N.C., Wulder, M.A., Vastaranta, M., Hilker, T., Tompalski, P., 2016. Remote sensing technologies for enhancing forest inventories: a review. Can. J. Remote. Sens. 42, 619–641.
Yamamoto, S.-I., 2000. Forest gap dynamics and tree regeneration. J. For. Res. 5, 223–229.
Zhang, K., 2008. Identification of gaps in mangrove forests with airborne LIDAR. Remote Sens. Environ. 112 (5), 2309–2325.
Zielewska-Büettner, K., Adler, P., Ehmann, M., Braunisch, V., 2016. Automated detection of forest gaps in spruce dominated stands using canopy height models derived from stereo aerial imagery. Remote Sens. 8, 175.
Zielewska-Büettner, K., Adler, P., Ehmann, M., Braunisch, V., 2017. Erratum: automated detection of forest gaps in spruce dominated stands using canopy height models derived from stereo aerial imagery. Remote Sens. 9 (5), 471.